Balanced boundary layers used in hurricane models

Roger K. Smith [a] *, and Michael T. Montgomery[b]

[a] *Meteorological Institute, University of Munich, Munich, Germany*
[b] *Dept. of Meteorology, Naval Postgraduate School, Monterey, CA & NOAA's Hurricane Research Division, Miami, FL, USA.*

Abstract:
We examine the accuracy of various approximations made in representing the boundary layer in simple axisymmetric hurricane models, especially those that assume *strict* gradient wind balance in the radial direction. Approximate solutions for a steady axisymmetric slab boundary layer model are compared with a full model solution. It is shown that the approximate solutions are poor in the inner core region of the vortex, where the radial acceleration is important and not generally negligible. These results have implications for a range of theoretical studies of hurricane dynamics that employ balanced boundary-layer formulations. Copyright © 2008 Royal Meteorological Society

1   Introduction

The boundary layer of a mature hurricane has been long recognized as an important feature of the storm. In particular, it controls the radial distribution of moisture, vertical motion and absolute angular momentum that ascends into the eyewall clouds. Early attempts to isolate the dynamics of the boundary layer of a mature hurricane were made by Rosenthal (1962) and Smith (1968). These studies highlighted a feature already well known from other areas of fluid dynamics that the boundary layer induces a secondary (overturning) circulation in the vortex above and that this circulation is associated with the imbalance of forces in the layer brought about by surface friction (see e.g. Greenspan 1968). A scale analysis of the boundary layer equations shows that the vertical gradient of perturbation pressure can be neglected to a first approximation so that the radial pressure gradient in the boundary layer is equal to that in the flow above the layer (see e.g. Vogl and Smith 2008). However, surface friction reduces the tangential wind speed and hence the centrifugal and Coriolis forces in the layer, leaving for a cyclonic vortex a net inward residual force. It is this net force that drives inflow in the layer, thereby inducing a secondary circulation in the vortex itself. Consistent with mass continuity, there is induced subsidence at outer radii and induced ascent at inner radii. In a hurricane, the inflowing air acquires moisture through evaporation at the sea surface and the moist air ascends to feed the eyewall clouds.

Despite that fact that the induced flow in the boundary layer is associated with gradient wind imbalance in the layer, many representations of the boundary layer have taken the tangential flow there to be in strict gradient

wind balance, but have included a sink of absolute angular momentum at the surface (Ogura 1964, Ooyama 1969, Schubert and Hack 1983, Emanuel 1986, 1989, 1995, 1997, 2004, Frisius 2005, 2006, Wirth and Dunkerton 2006). We are unaware of any reasoned justification for such a formulation, but one could imagine that the dynamics of the hurricane boundary layer is essentially different from that in which friction plays an active role, since any inflow in these balance models cannot be "driven" directly by frictional imbalance. At best they may be expected to be a valid first approximation only where the radial flow is sufficiently slow. A natural questions then arises, how severe are their limitations? We have shown recently (Smith et al. 2008) that the assumption of balance is poor in Emanuel's steady-state hurricane model (Emanuel 1986) and by implication in his theory for potential intensity (Emanuel 1995, Bister and Emanuel 1998).

Two of the early pioneering models of hurricanes, those of Ooyama (1969) and Sundqvist (1970), were balanced in the sense that the tangential, or primary circulation was taken to be in gradient wind balance, and both models were considered to produce reasonably realistic simulations of hurricanes. Indeed, the gradient balance assumption is thought to be a relatively accurate one over most of the free troposphere, except in the upper-level outflow layer, and the assumption is supported by an elementary scale analysis for a rapidly-rotating vortex in which the radial component of flow is much less than the tangential component (Willoughby 1979). It is supported also by aircraft reconnaisance measurements in the lower troposphere (Willoughby 1977). These early models assumed, however, that the boundary layer is also in gradient wind balance. Ooyama was aware of the limitations of the latter assumption and wrote in an unpublished manuscript in 1968 " ... it appears that the weakest hypothesis in the original model is the use of

---

*Correspondence to: Roger K. Smith, Meteorological Institute, University of Munich, Theresienstr. 37, 80333 Munich, Germany. E-mail: roger.smith@lmu.de

the balance approximation in the boundary layer". In the manuscript, Ooyama went on to show that the solutions in a calculation with a more complete boundary layer formulation were more realistic than those with a balanced boundary-layer formulation. As far as we are aware, most authors have not seriously questioned the accuracy of the balanced assumption in the hurricane boundary layer, even though a scaling analysis of the layer (Smith 1968, Vogl and Smith 2008) shows that it is unlikely to be an accurate approximation in the inner core boundary layer of a hurricane vortex, a finding supported also by more recent numerical simulations of hurricanes (Persing and Montgomery 2003, Appendix; Kepert and Wang 2001).

In this paper we compare the predictions of various approximate formulations of the boundary layer in a steady slab model, including those that assume gradient wind balance, with that of a unapproximated formulation. Using the unapproximated solution as a control, we examine the accuracy of the various approximate formulations. We begin by examining the features of balanced models in general, reviewing the role of friction in the secondary circulation as described by the Sawyer-Eliassen equation.

2 Balanced hurricane models

The cornerstone of all balance theories for vortex evolution is the Sawyer-Eliassen (SE-) balance model which describes the slow evolution of an axisymmetric vortex forced by heat and (azimuthal) momentum sources. Here the flow is assumed to be axisymmetric and in strict gradient wind and hydrostatic balance. We summarize the SE model here for the simplest configuration, namely the axisymmetric flow of an incompressible Boussinesq fluid with constant ambient Brunt-Väisälä frequency, N. The hydrostatic primitive equations of motion may be expressed in cylindrical polar coordinates (r, λ, z) as

$$\frac{\partial u}{\partial t} + u\frac{\partial u}{\partial r} + w\frac{\partial u}{\partial z} - C = -\frac{\partial P}{\partial r} + F_r, \qquad (1)$$

$$\frac{\partial v}{\partial t} + u\frac{\partial v}{\partial r} + w\frac{\partial v}{\partial z} + \frac{uv}{r} + fu = F_\lambda, \qquad (2)$$

$$0 = \frac{\partial P}{\partial z} + b, \qquad (3)$$

$$\frac{\partial \sigma}{\partial t} + u\frac{\partial \sigma}{\partial r} + w\frac{\partial \sigma}{\partial z} + N^2 w = \dot{B}, \qquad (4)$$

$$\frac{\partial ru}{\partial r} + \frac{\partial rw}{\partial z} = 0, \qquad (5)$$

where (u, v, w) is the velocity vector in this coordinate system, $C = v^2/r + fv$ is the sum of the centrifugal and Coriolis terms, $P = p/\bar{\rho}$ is the pressure p divided by the mean density $\bar{\rho}$, σ is the buoyancy force, $\dot{B}$ is the diabatic source of buoyancy, and F_r and F_λ are the radial and tangential components of frictional stress, respectively.

With the additional assumption of gradient wind balance, Eq. (1) reduces to

$$C = \frac{\partial P}{\partial r}. \qquad (6)$$

If P is eliminated by cross-differentation with the hydrostatic equation (3), we obtain the thermal wind equation

$$\frac{\partial \sigma}{\partial r} = -\xi\frac{\partial v}{\partial z}, \qquad (7)$$

where $\xi = 2v/r + f$. The SE equation is obtained by differentiating (7) with respect to time, eliminating the time derivatives of v and σ using Eqs. (2) and (4) and introducing a streamfunction ψ for the secondary circulation such that the continuity equation (5) is satisfied, i.e. we write $u = -(1/r)(\partial\psi/\partial z)$ and $w = (1/r)(\partial\psi/\partial r)$. Then, with a little algebra we obtain:

$$\frac{\partial}{\partial r}\left[\left(N^2 + \frac{\partial\sigma}{\partial z}\right)\frac{1}{r}\frac{\partial\psi}{\partial r} - \frac{\partial}{\partial z}\left(\frac{S\xi}{r}\frac{\partial\psi}{\partial z}\right)\right] +$$
$$\frac{\partial}{\partial z}\left[\frac{\xi\zeta_a}{r}\frac{\partial\psi}{\partial z} - \frac{\xi S}{r}\frac{\partial\psi}{\partial r}\right] = \frac{\partial\dot{B}}{\partial r} - \frac{\partial}{\partial z}(\xi F_\lambda), \qquad (8)$$

where $S = \partial v/\partial z$ is the vertical wind shear and $\zeta_a = (1/r)(\partial rv/\partial r)$ is the absolute vorticity. More general derivations of this equation are found, for example, in Willoughby (1979), Shapiro and Willoughby (1982) and Smith et al. (2005). The SE-equation is elliptic if the vortex is symmetrically stable (i.e. if the inertial stability on isentropic surfaces is greater than zero). It is readily shown that symmetric stability is assured when $(N^2 + \partial\sigma/\partial z)\zeta_a\xi - (\xi S)^2 > 0$ (Shapiro and Montgomery 1993). Given suitable boundary conditions this equation may be solved for the streamfunction of the secondary circulation ψ at a given time. Being a balance model only one prognostic equation is used to advance the system forward in time. The set of equations (2) (or (4)), (7) and (8) thus provide a system that can be solved for the balanced evolution of the vortex. Equation (2) (or (4)) along with the diagnostic equation (7) is used to predict the future state of the primary circulation with values of u and w at a given time being computed from the streamfunction ψ obtained by solving Eq. (8). The secondary circulation given by (8) is just that required to keep the primary circulation in hydrostatic and gradient wind balance in the presence of the processes trying to drive it out of balance. These processes are represented by the radial gradient of the rate of buoyancy generation and the vertical gradient of ξ times the tangential component of frictional stress. It follows that surface friction can induce radial motion in a balanced formulation of the boundary layer.

The Sawyer-Eliassen equation can be simplified by using potential radius coordinates in which the radius r is replaced by the potential radius, R, defined by $\frac{1}{2}fR^2 = rv + \frac{1}{2}fr^2$, the right-hand-side being the absolute angular momentum (Schubert and Hack 1983). In this case surfaces of absolute angular momentum are vertical and the assumption that these surfaces are coincident with the moist isentropes provides an elegant way to formulate the zero-order effects of moist convection (Emanuel 1986, 1989, 1995, 1997). It is for this reason, perhaps, that balanced models remain popular. Nevertheless, the question remains whether the boundary layer in such models

is sufficiently accurate? We explore this question below in the context of a simple slab formulation for the boundary layer and approximations thereto.

3 A slab model for the boundary-layer

We review first the slab boundary layer model described by Smith and Vogl (2008: henceforth SV08), which provides a suitable framework to examine the accuracy of various approximations in boundary-layer formulations. For simplicity we assume the boundary layer to have uniform depth[†], h, and constant density. In our cylindrical coordinate system, the vertically-integrated equations for the radial momentum, azimuthal momentum and mass continuity can be written in the following form:

$$u_b \frac{du_b}{dr} = \frac{w_{h-} + w_{sc}}{h} u_b - \frac{(v_{gr}^2 - v_b^2)}{r} - f(v_{gr} - v_b)$$
$$- \frac{C_D}{h}(u_b^2 + v_b^2)^{\frac{1}{2}} u_b, \qquad (9)$$

$$u_b \frac{dv_b}{dr} = \frac{w_{h-} + w_{sc}}{h}(v_b - v_{gr}) - (\frac{v_b}{r} + f)u_b$$
$$- \frac{C_D}{h}(u_b^2 + v_b^2)^{\frac{1}{2}} v_b, \qquad (10)$$

$$\frac{du_b}{dr} = -\frac{u_b}{r} - \frac{w_h}{h}, \qquad (11)$$

where u_b and v_b are the vertically-averaged radial and azimuthal components of wind speed in the boundary layer, $v_{gr}(r)$ and w_h are the tangential wind speed and vertical velocity at the top of the boundary layer, f is the Coriolis parameter, C_D is the surface drag coefficient and $w_{h-} = \frac{1}{2}(w_h - |w_h|)$. The terms involving w_{sc} represent turbulent fluxes at the top of the boundary layer (arising from rainbands, shallow convection, or smaller-scale turbulent structures), but for simplicity we do not consider them here, setting w_{sc} equal to zero. Consistent with the slab formulation, the quantities u_b and v_b are assumed to be independent of depth. Note that w_{h-} is nonzero only when $w_h < 0$, in which case it is equal to w_h. Thus the terms involving w_{h-} represent the transport of properties from above the boundary layer that may be different from those inside the boundary layer. As in SV08 we take $C_D = C_{D0} + C_{D1}|\mathbf{u_b}|$, where $C_{D0} = 0.7 \times 10^{-3}$ and $C_{D1} = 6.5 \times 10^{-5}$ for wind speeds less than 20 m s^{-1} and $C_D = 2.0 \times 10^{-3}$, a constant, for larger wind speeds. These values are based on our interpretation of Fig. 5 from Black et al. (2007).

Substitution of Eq. (11) into Eq. (9) gives an expression for w_h:

$$w_h = \frac{h}{1+\alpha}\left[\frac{1}{u_b}\left(\frac{v_{gr}^2 - v_b^2}{r} + f(v_{gr} - v_b)\right.\right.$$
$$\left.\left. + \frac{C_D}{h}(u_b^2 + v_b^2)^{\frac{1}{2}} u_b\right) - \frac{u_b}{r}\right], \qquad (12)$$

[†]SV08 considered also the variable depth case, but for simplicity the focus here is on the constant depth boundary layer assumed by Emanuel (1986).

where α is zero if the expression in square brackets is positive and unity if it is negative. With this expression for w_h, Eqs. (9), (10) and (12) form a system of ordinary differential equations that may be integrated radially inwards from some large radius R to determine u_b and v_b as functions of r, given values of these quantities at $r = R$ as well as the radial profile $v_{gr}(r)$.

We discuss now various rational approximations possible to the foregoing equations as discussed below.

3.1 Linear approximation

A common simplification of the full boundary-layer equations is to neglect the terms involving the vertical advection through the top of the layer and to linearize Eqs. (9) and (10), treating the magnitudes of u_b and $v' = v - v_{gr}$ as small compared with v_{gr} (Eliassen and Lystad 1977, Kepert 2001). The linearized boundary layer equations then become

$$\xi(v_{gr} - v_b) = -\frac{C_D}{h}(u_b^2 + v_b^2)^{\frac{1}{2}} u_b, \qquad (13)$$

$$\zeta_a u_b = -\frac{C_D}{h}(u_b^2 + v_b^2)^{\frac{1}{2}} v_b, \qquad (14)$$

where ξ and ζ_a are as defined in section 2. The equations may be solved locally for u_b and v_b in terms of v_{gr}, ξ and ζ_a, the last two quantities being calculated from v_{gr}. It is convenient to write $(u_b, v_b) = v_{gr}(bu, v)$, where $b^2 = \xi/\zeta_a$. Dividing (13) by (14) and rearranging gives the equation for an circle

$$u^2 + \left(v - \frac{1}{2}\right)^2 = \frac{1}{4}. \qquad (15)$$

Also, squaring Eq. (14) gives a second equation relating u and v:

$$v = +b\left(\left\{\frac{1}{4}u^4 + \frac{c^2}{b^2}u^2\right\}^{\frac{1}{2}} - \frac{1}{2}u^2\right)^{\frac{1}{2}}, \qquad (16)$$

where $c = h\zeta_a/(C_d v_{gr})$.

Families of curves given by (15) and (16) for typical values of the parameters b and c are shown in Fig. 1 (see section 4. The intersections of these curves in the region $u < 0, v > 0$ (assuming a cyclonic vortex for v_{gr}) give the required solutions for (u, v) and hence for (u_b, v_b). These solutions may be readily obtained by a simple Newton-Rapheson algorithm as explained in SV08 (see appendix therein). The fact that all solutions for (u, v) lie on a circle of radius one half implies a bound on the magnitude of the ratios $bu = u_b/v_{gr}$ and $v = v_b/v_{gr}$, which may not exceed $\frac{1}{2}b$ and unity, respectively. Therefore the occurrence of supergradient winds is ruled out in these linear depth-averaged formulations, but u_b could exceed v_{gr} if b is sufficiently large.

Despite this ability to obtain a solution to the linearized equations with the quadratic friction terms intact, one might argue that a consistent formulation of the linearized equations would include also a linearization of the
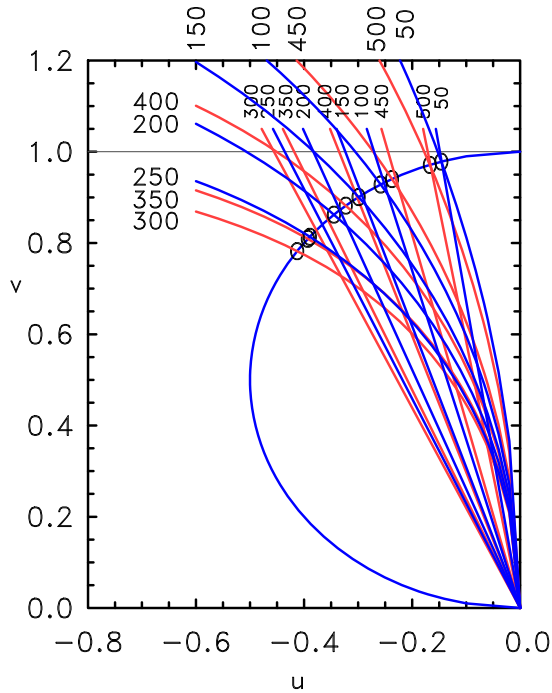
Figure 1. The circle corresponding with Eq. (15) and the curves given by Eq. (16) for typical values of the parameters b and c derived from the radial profile of v_{gr} used to construct Fig. 2. The straight lines are those given by Eq. (17) for the same parameters. The numbers marking the curves are the radii in km at which the parameters b and c are calculated. Blue curves correspond to radii ≤ 250 km and red curves for radii ≥ 300 km.

friction terms, approximating $(u_b^2 + v_b^2)^{1/2}$ by v_{gr}. In this case, Eq. (15) does not change, but Eq. (16) becomes simply

$$v = -\mu u, \qquad (17)$$

where $\mu = bc = hI/(C_d v_{gr})$ and I is defined by $I^2 = \xi \zeta_a$. The straight lines represented by Eq. (17) are shown also in Fig. 1. The intersection of these lines with the corresponding circle gives the solution for u and v when the quadratic terms in Eqs. (13) and (14) are linearized. Note that there are moderate differences between the solutions with and without the linearization of the friction terms for most values of the parameters.

If in addition to the linear approximation we make the small Rossby number assumption, ξ and ζ_{agr} may both be approximated by f. Then Eqs. (13) and (14) become the slab equivalent of the Ekman layer equations. In this case, $b = 1$ so that $(u_b, v_b) = v_{gr}(u, v)$, while c in (16) reduces to $c_g = hf/(C_d v_{gr})$.

3.2 Balanced approximation

If we make the strict gradient wind balance approximation as well as the linear approximation, i.e. if we assume that the tangential wind speed in the boundary layer is equal to that above, Eq. (13) is by necessity trivial

$$v_{gr} = v_b, \qquad (18)$$

and Eq. (14) gives directly an expression for the radial wind speed, i.e.

$$\zeta_a u_b = -\frac{C_D}{h}(u_b^2 + v_{gr}^2)^{\frac{1}{2}} v_{gr}, \qquad (19)$$

whereupon

$$u_b = -v_{gr}\left(\frac{1}{c^2 - 1}\right)^{\frac{1}{2}}. \qquad (20)$$

3.3 Emanuel's balanced approximation

Emanuel (1986) made the additional assumption that the radial wind component can be neglected when calculating the total wind speed in the friction term. In this case the radial wind speed is given by

$$u_b = -\frac{1}{c}v_{gr}, \qquad (21)$$

which is similar to the dimensional form of Eq. (17) except that v_b is approximated by v_{gr}.

4 Some solutions

In this section we assess the accuracy of the linear and balanced approximations made in subsections 3.1, 3.2 and 3.3 by comparing the solutions of these systems with that from the full equations (9), (10) and (12), which we refer to as the control calculation. The profile of v_{gr} is the same as that used in SV08, i.e. $v_{gr} = v_1 s \exp(-\alpha_1 s) + v_2 s \exp(-\alpha_2 s)$, where $s = r/r_m$ and r_m the radius at which the tangential wind speed is a maximum and equal to v_m. In the calculations here, v_m and r_m are taken to be 40 m s^{-1} and 40 km, respectively corresponding with the values: $\alpha_1 = 1.4118$, $\alpha_2 = 0.3$, $v_1 = 103.34$ and $v_2 = 20.0$. The Coriolis parameter is taken to be $f = 5 \times 10^{-5}$ s^{-1}. The geostrophic solution is used to initialize the control calculation at a radius of 500 km, where the local Rossby number $v_{gr}(R)/(fR) = 0.24$ is small enough for the geostrophic solution to be reasonably accurate (here $v_{gr}(R) = 5.88$ m s^{-1}.

4.1 Constant depth boundary layer

The results of the various calculations are summarized in Fig. 2 for a boundary layer with a constant depth of 800 m. The figure shows radial profiles of (inward) radial and tangential wind components in the boundary layer and the vertical velocity component at the top of the boundary layer. The latter is calculated analytically from Eq. (12) for the control calculation and from the continuity equation (11) for the approximations to it. Figure 2 shows also the profile of tangential wind assumed at the top of the boundary layer (v_{gr}) and the radial variation of the parameters b in Eq. (15) and c in Eqs. (16) and (21).

The behaviour of all solutions shows an increase in v_b with decreasing radius together with an increase in the magnitude of u_b down to a radius of 47 km in the case of v_b and 84 km in the case of u_b. In
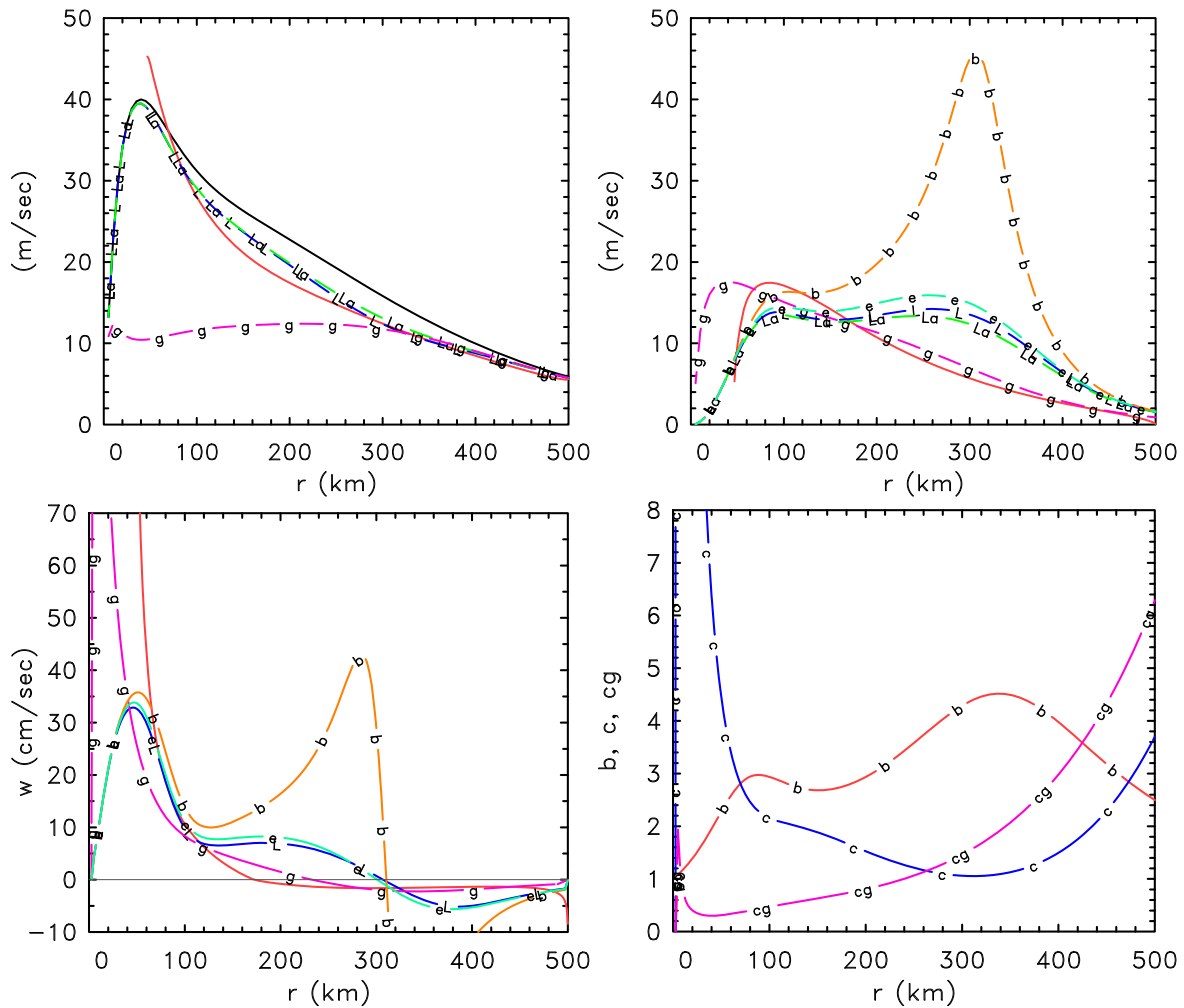
Figure 2. Radial profiles of: (a) tangential, and (b) radial wind components in the slab boundary layer calculation described in section 3 and in the various approximations to it. The solid black line is the assumed tangential wind profile at the top of the boundary layer, v_{gr} and the solid red line is the unapproximated boundary layer solution. [Units m s^{-1}] For plotting convenience the sign of u_b has been reversed. "L" represents the linear solution, "La" the linear solution with the friction terms linearized, "g" the geostrophic solution, "b" the balanced solution and "e" Emanuel's balanced approximation. (c) The corresponding profiles of vertical motion at the top of the boundary layer. (d) The radial variation of the parameters b, c and c_g (labelled "cg") for the assumed tangential wind profile.

the control solution, the tangential wind speed becomes supergradient ($v_b > v_{gr}$) in the inner core region ($r < 69$ km) and because of this, the radial flow suffers a rapid deceleration (SV08). In contrast, all the approximate solutions remain subgradient. The tangential wind speed in the linear and geostrophic solutions is close to that in the control calculation at radii larger than about 300 km, but the geostrophic solution shows a very large deviation from it at smaller radii. In contrast, the radial wind in the geostrophic calculation follows the control rather closely except at radii less than 100 km, whereas that in the linear and Emanuel balanced approximations show a significant deviation from the control at most radii, being significant overestimates at radii between about 200 km and 400 km and moderate underestimates at radii around 100 km. The balance approximation in subsection 3.2 shows an enormous deviation from other solutions, a feature that is attributed to the fact that, at least for the profile chosen for v_{gr}, the parameter c in (20) approaches unity so that the denominator in Eq. (20) becomes relatively large

(Fig. 2d). Emanuel's balanced approximation is superior in this respect and the radial wind remains close to the linear solution at all radii, although like the latter, it shows significant departures from the control calculation. There is very little difference between the radial and tangential wind components in linear calculation and the form thereof in which the friction term is linearized.

There are significant differences in the vertical velocity between the various approximations and the control calculation. The control calculation breaks down at a radius of about 50 km where the radial wind speed tends to zero. This behaviour is not replicated by any of the other solutions. At slightly larger radii, the vertical velocity in the control calculation increases rapidly with decreasing radius, but where there are large radial gradients, the approximations on which boundary-layer theory is based will no longer be valid. Again, the balanced solution shows a large deviation compared with all other solutions between about 200 and 400 km radius. The geostrophic solution predicts large vertical velocities at small radii,
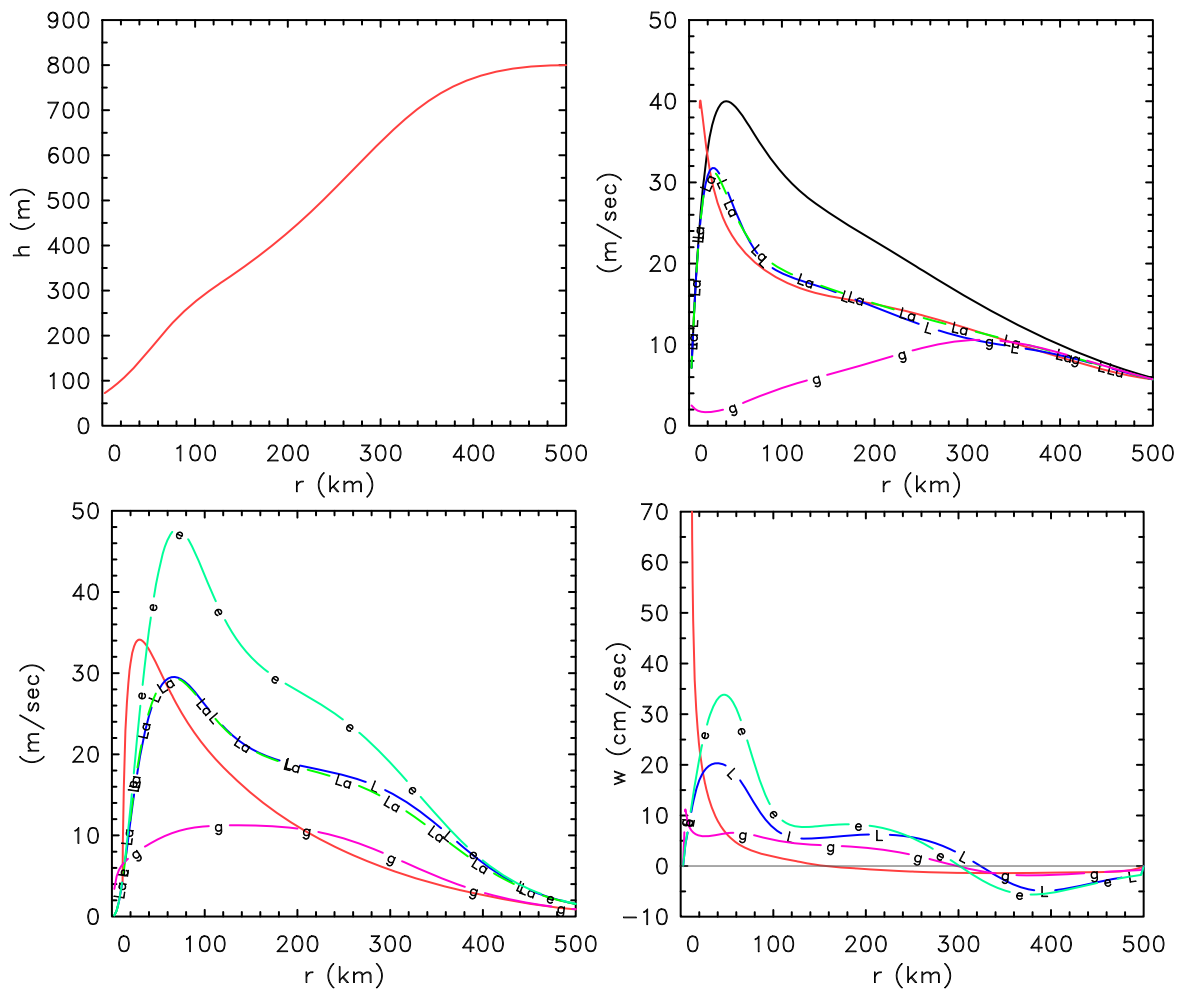
Figure 3. Calculations with variable boundary layer depth. Radial profiles of: (a) assumed boundary layer depth, (b) tangential, and (c) radial wind components in the slab boundary layer calculation described in section 3 and in the various approximations to it. The solid black line is the assumed tangential wind profile at the top of the boundary layer, v_{gr} and the solid red line is the unapproximated boundary layer solution. [Units m s^{-1}] For plotting convenience the sign of u_b has been reversed. "L" represents the linear solution, "La" the linear solution with the friction terms linearized, "g" the geostrophic solution, "b" the balanced solution and "e" Emanuel's balanced approximation. (d) The corresponding profiles of vertical motion at the top of the boundary layer.

while the linear solution and Emanuel's balanced approximation show a maximum vertical velocity of about 35 cm s^{-1} at a radius of about 60 km. There are significant differences also between the radii at which the vertical velocity changes sign, this being about 170 km in the control calculation, 235 km in the geostrophic calculation, 300 km in Emanuel's balanced calculation and 310 km in the large-discrepancy balanced calculation.

5 Solutions for radially-varying layer depths

A scale analysis of the boundary layer equations indicate that the boundary-layer depth is inversely proportional to the square root of the inertial stability, I, at the top of the boundary layer. This scaling would imply a significant reduction in depth between the starting radius and the core region (see e.g. Fig. 3a). Such a variation is supported by the linear solution to the full boundary-layer equations that accounts for vertical structure of the layer (Eliassen and Lystad 1977, Kepert 2001) as well as full numerical

solutions (Kepert and Wang 2001, Montgomery et al. 2001). While it is not possible to determine the radial variation of δ in the slab-model, it is straightforward to modify Eqs. (9) - (12) to allow for a prescribed variation $\delta(r)$ (see SV08, Appendix A). To assess the effect of a decrease in δ with declining radius we carried out calculations in which $\delta(r) = \delta(R)\sqrt{(I_g/I)}$, where $\delta(R)$ is the boundary layer depth at $r = R$ and I_g is the value of I at this radius. The solutions for $\delta(R) = 800$ m are shown in Fig. 3. In the control calculation the tangential wind speeds in the boundary layer are decreased, especially inside a region of about 200 km and the peak winds are significantly lower in magnitude than v_m. In contrast the peak radial winds are significantly larger than in the constant-depth calculations and the maximum occurs at markedly smaller radius. When the boundary-layer depth decreases with decreasing radius, the maximum vertical velocity at the top of the layer is reduced considerably from that in the constant-depth calculations and is more in line with that in previous calculations (e.g. Kepert and
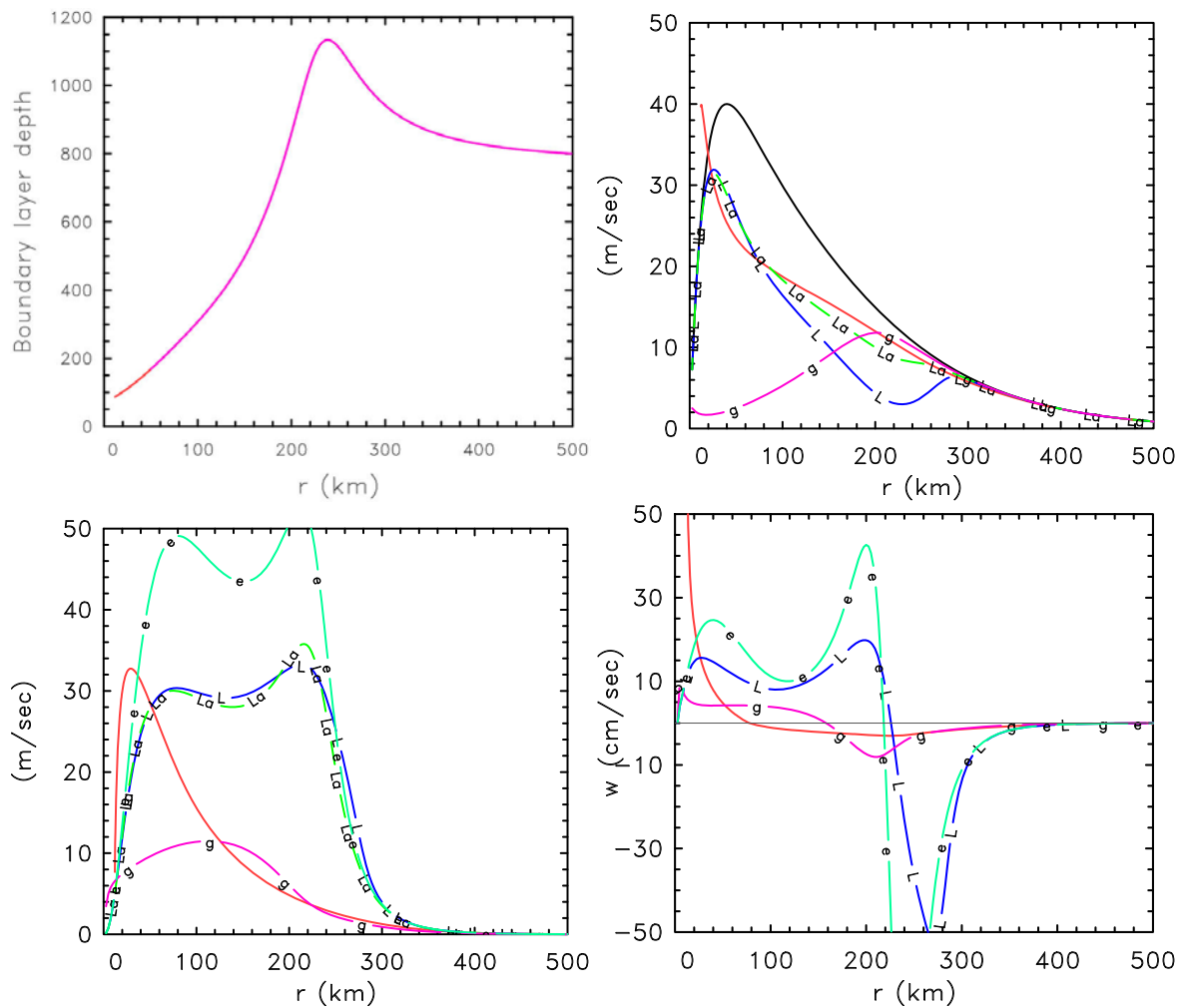
Figure 4. Legend as for Fig. 3, but for a narrower vortex profile.

Wang 2001: see e.g. their Fig. 3). The variable-depth calculations still show supergradient wind speeds, but now well inside r_m in a region where radial gradients are probably steep enough to strain the assumptions of boundary layer theory. We have puposely omitted to show the balanced solution of section 3.2 in Fig. 3 as the parameter c^2 in Eq. (20) has values less than unity over a large range of intermediate radii. At these radii, the balanced solution does not exist for the particular v_{gr} profile used.

The linear approximation, that with linear friction, and the Emanuel balanced approximation predict the tangential wind speed rather well, almost up to the radius at which the tangential wind component becomes supergradient in the control calculation. The geostrophic approximation remains accurate inwards to a radius of about 300 km, but greatly undersetimates the tangential wind component inside this radius. The predictions of the radial wind component by the approximate theories are all poor in comparison to that in the control calculation, except, surprisingly that of the geostrophic approximation at radii larger than about 200 km. Inside this radius, however, the geostrophic approximation is poor also. The Emanuel balanced approximation gives by far the worst prediction of

the radial component with a maximum exceeding that of the control calculation by 10-20 m s^{-1} at radii between about 70 km and 300 km. Note that in this approximation, the radial wind is just minus the ratio of the tangential wind above the boundary layer divided by the profile-dependent parameter c. All the approximate theories overestimate the subsidence into the boundary layer at outer radii (≥ 320 km) and show ascent occurring inside this radius compared with a radius of 160 km in the control. Moreover the ascent is much larger than in the control except within a radius of about 30 km.

Figure 4 shows plots analogous to those in Fig. 3, but for a narrower vortex profile that has the same values of r_m and v_m (the functional form is the same as before, but $v_1 = 90.06$ m s^{-1}, $v_2 = 36$ m s^{-1}, $\alpha_1 = 1.601$, $\alpha_2 = 0.5$). The radius of gale-force winds (17 m s^{-1}) is 317 km compared with 381 km in Fig. 3. For this profile, the inertial stability parameter, I, has a local minimum at a radius of about 240 km, which implies a local maximum in the boundary-layer depth at this radius (Fig. 4a). Because the radial gradients are larger, one would expect a narrow vortex profile to strain the balanced approximations more than a broader one and this expectation is confirmed
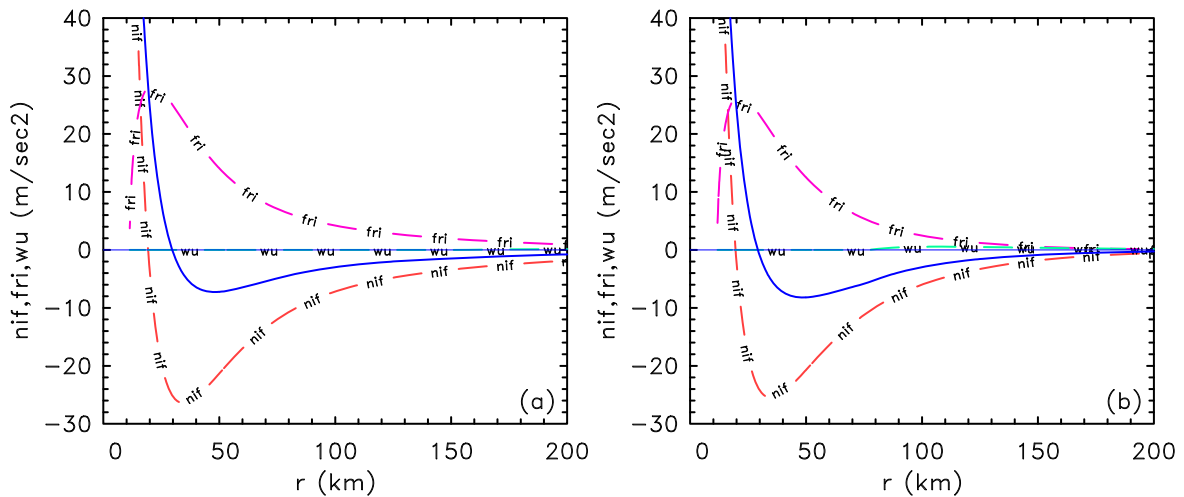
Figure 5. Contributions to the radial momentum balance for radii less than 200 km in the variable depth calculations in (a) Fig. 3, and (b) the narrower vortex profile in Fig. 4. The labelling on the curves refers to the net inward force (nif), the frictional force (fri), the vertical advection of momentum into the boundary layer (wu) and the residual force, the solid blue line.

by the solutions. Now the full linear balanced approximation is the worst of all of the approximations in capturing the tangential wind component in the boundary layer at radii between 60 km and 300 km. In contrast, the version with linear friction and Emanuel's balanced approximation being reasonably accurate until near the radius at which the tangential wind component in the control calculation becomes supergradient. However the radial wind component is greatly overestimated by all the approximations at a radii less than about 320 km, with again the Emanuel balanced calculation being the least accurate. The vertical velocity at the top of the boundary layer is likewise very poor compared with that in the control calculation and worse than in the broader tangential wind profile in Figs. 2 and 3.

    The reasons for the large deviations of the radial and vertical winds in the balance solutions from those in the control calculation may be inferred from Fig. 5, which shows the radial force fields for the two vortex profiles in the calculations with variable boundary-layer depth. The net inward driving force, the difference between the inward pressure gradient force and the outward-directed centrifiugal and Coriolis forces, exceeds the frictional force by a significant fraction leaving a net inward force which is just the radial acceleration. This net inward force is appreciable down to the radius just inside r_m, when it begins to decrease rapidly, reversing sign about 10 km outside the radius at which the net driving force changes sign and the tangential wind component becomes supergradient. The foregoing remarks apply to both panels in Figs. 5 and, as expected, the radial acceleration is a little larger for the narrower vortex profile.

6   Conclusions

Our calculations for the chosen tangential wind profiles v_{gr} show that the linear solution and Emanuel's balanced version thereof tend to overestimate the inflow in the

boundary layer at large radii ($\geq$ 160 km) and underestimate it at inner radii. They predict the maximum vertical motion to occur at an unrealistically large radius (more than 250 km) and they are unable to capture the formation of supergradient winds. We consider such formulations to be inappropriate for representing the boundary layer in the inner core region of a hurricane. The balanced formulation without a linearization of the friction term is especially unrealistic.

7   Acknowledgements

References

Black, P. G., D'Asaro, E. A., Drennan, W. M., French, J. R., Niiler, P. P., Sanford, T. B., Terrill, E. J., Walsh, E. J. and J. A. Zhang 2006 Air-sea exchange in hurricanes: Synthesis of observations from the coupled boundary layer air-sea transfer experiment. *Bull. Amer. Meteor. Soc.*, **88**, 357-374

Eliassen, A. and M. Lystadt 1977 The Ekman layer of a circular vortex: A numerical and theoretical study. *Geophysica Norvegica*, **31**, 1-16

Emanuel, K. A. 1986 An air-sea interaction theory for tropical cyclones. Part I: Steady-state maintenance. *J. Atmos. Sci.*, **43**, 585-604

Emanuel, K. A. 1988 The maximum intensity of hurricanes. *J. Atmos. Sci.*, **45**, 1143-1155

Emanuel, K. A. 1989 The finite-amplitude nature of tropical cyclogenesis. *J. Atmos. Sci.*, **46**, 3431-3456

Emanuel, K. A. 1995 Sensitivity of tropical cyclones to surface exchange coefficients and a revised steady state model incorporating eye dynamics. *J. Atmos. Sci.*, **52**, 3969-3976

Emanuel, K. A. 1997 Some aspects of hurricane inner-core dynamics and energetics. *J. Atmos. Sci.*, **54**, 1014-1026

Emanuel, K. A. 2004 Tropical cyclone energetics and structure. In *Atmospheric Turbulence and Mesoscale Meteorology*, Eds. E. Fedorovich, R. Rotunno and B. Stevens, Cambridge University Press, London, 280 pp

Frisius, T. 2005 An atmospheric balanced model of an axisymmetric vortex with zero potential vorticity. *Tellus*, **57,** 5564

Frisius, T. 2006 Surface-flux-induced tropical cyclogenesis within an axisymmetric atmospheric balanced model. *Quart. J. Roy. Meteor. Soc.*, **132,** 26032623

Greenspan, H. P., 1968 *Theory of rotating fluids*. Cambridge University Press, London, ppXXX

Kepert, J. D. 2001 The dynamics of boundary layer jets within the tropical cyclone core. Part I: Linear Theory. *J. Atmos. Sci.*, **58,** 2469-2484

Kepert, J. D. and Y. Wang 2001 The dynamics of boundary layer jets within the tropical cyclone core. Part II: Nonlinear enhancement. *J. Atmos. Sci.*, **58,** 2485-2501

Montgomery, M. T., Snell, H. D. and Z. Yang 2001 Axisymmetric spindown dynamics of hurricane-like vortices. *J. Atmos. Sci.*, **58,** 421-435

Ooyama, K. V. 1969 Numerical simulatoion of the life-cycle of tropical cyclones. *J. Atmos. Sci.*, **26,** 3-40

Persing, J., and M. T. Montgomery 2003 Hurricane superintensity. *J. Atmos. Sci.*, **60,** 2349-2371

Rosenthal, S. L. 1962 A theoretical analysis of the field motion in the hurricane boundary layer. *National Hurricane Research Project Report No 56*, US Dept of Commerce, 12pp

Schubert, W. H., and J. J. Hack 1999 Transformed Eliassen balanced vortex model. *J. Atmos. Sci.*, **40,** 1571-1583

Shapiro, L. J., and M. T. Montgomery 1993 A three-dimensional balance theory for rapidly rotating vortices. *J. Atmos. Sci.*, **50,** 3322-3335

Shapiro, L. J. 1983 The asymmetric boundary layer under a translating hurricane. *J. Atmos. Sci.*, **40,** 1984-1998

Shapiro, L. J., and H. Willoughby 1982 The response of balanced hurricanes to local sources of heat and momentum. *J. Atmos. Sci.*, **39**, 378-394

Smith, R. K. 1968 The surface boundary layer of a hurricane. *Tellus*, **20**, 473-483

Smith, R. K., 2003 A simple model of the hurricane boundary layer. *Quart. J. Roy. Meteor. Soc.*, **129**, 1007-1027

Smith, R. K., and S. Vogl 2008 A simple model of the hurricane boundary layer revisited. *Quart. J. Roy. Meteor. Soc.*, **134**, In press

Smith, R. K., M. T. Montgomery, and H. Zhu 2005 Buoyancy in tropical cyclones and other rapidly rotating vortices. *Dyn. Atmos. Oceans,* **40,** 189-208

Smith, R. K., M. T. Montgomery, and S. Vogl 2008 A critique of Emanuel's hurricane model and potential intensity theory. *Quart. J. Roy. Meteor. Soc.,* **134**, revised version submitted Jan 2008

Sundqvist, H. K. 1970 Numerical simulation of the development of a hurricane in a ten level model. *Tellus*, **22**, 359-390

Vogl, S., and Smith, R. K. 2008 Eliassen's linear model for a vortex boundary layer applied to a hurricane. *Quart. J. Roy. Meteor. Soc.*, **134**, to be submitted Feb 2008

Willoughby, H. E., 1990 Gradient balance in tropical cyclones. *J. Atmos. Sci.*, **47**, 465-489

Willoughby, H. 1979 Forced secondary circulations in hurricanes. *J. Geophys. Res.*, **84**, 3173-3183

Wirth, V., and T. J. Dunkerton 2006 A unified perspective on the dynamics of hurricanes and monsoons. *J. Atmos. Sci.*, **63**, 2529-2547